ISSN 2072-5981
doi: 10.26907/mrsej

Magnetic Resonance in Solids

Electronic Journal

Volume ***26***

Issue ***2***

Article No ***24207***

1-6 pages

June, ***6***

2024

doi: **10.26907/mrsej-24207**

http://mrsej.kpfu.ru

https://mrsej.elpub.ru

Established and published by Kazan University*
Endorsed by International Society of Magnetic Resonance (ISMAR)
Registered by Russian Federation Committee on Press (#015140),
August 2, 1996
First Issue appeared on July 25, 1997

"***Magnetic Resonance in Solids. Electronic Journal***" (**MRSej**) is a peer-reviewed, all electronic journal, publishing articles which meet the highest standards of scientific quality in the field of basic research of a magnetic resonance in solids and related phenomena.

Indexed and abstracted by
Web of Science (*ESCI*, Clarivate Analytics, from 2015),
Scopus (Elsevier, from 2012), *RusIndexSC* (*eLibrary*, from 2006), *Google Scholar*,
DOAJ, *ROAD*, *CyberLeninka* (from 2006), *SCImago Journal & Country Rank*, etc.

* Address: "Magnetic Resonance in Solids. Electronic Journal", Kazan Federal University; Kremlevskaya str., 18; Kazan 420008, Russia
† In Kazan University the Electron Paramagnetic Resonance (EPR) was discovered by Zavoisky E.K. in 1944.
‡ Dedicated to Professor Boris Z. Malkin on the occasion of his 85th birthday

Rabi oscillations and ENDOR study of trivalent gadolinium ion in $LiYF_4$ crystal

G.V. Mamin, F.F. Murzakhanov, I.N. Kurkin, M.R. Gafurov, E.I. Baibekov*

Kazan Federal University, Kazan 420008, Russia

**E-mail: edbaibek@gmail.com*

(Received June 5, 2024; accepted June 5, 2024; published June 6, 2024)

We demonstrate coherent electron and electron-nuclear spin manipulations using the impurity trivalent gadolinium ion and the nearby ^{7}Li and ^{19}F nuclei incorporated in the $LiYF_4$ host crystal. In particular, we present the electronic Rabi oscillations corresponding to $-1/2 \leftrightarrow 1/2$ and $5/2 \leftrightarrow 7/2$ transitions between the projections of the Gd^{3+} spin $S = 7/2$ of the lowest manifold $^8S_{7/2}$, together with the spin-lattice and spin-spin coherence times of these transitions. High-resolution pulsed electron-nuclear double resonance spectra involving $-1/2 \leftrightarrow 1/2$ or $5/2 \leftrightarrow 7/2$ gadolinium transitions and either ^{7}Li (nuclear spin $I = 3/2$) or ^{19}F ($I = 1/2$) nuclear spin transition are obtained. The results suggest that the particular system can be potentially used for the implementation of hybrid quantum calculations utilizing both the electronic high-spin gadolinium states and the nuclear spin states of the adjacent ions.

PACS: 76.30.-v, 76.30.Kg, 76.70.Dx, 03.67.Lx.

Keywords: Rabi oscillations, ENDOR, EPR, gadolinium, $LiYF_4$.

Dedicated to Boris Malkin, an outstanding teacher and colleague, on the occasion of his 85th birthday

1. Introduction

Localized electron spins in a solid are potential qubits for quantum information processing [1], since they provide opportunities for scaling and have long coherence times (up to several milliseconds). Among possible implementations are rare earth ions diluted in single crystals [2]. Boris Malkin is a person who initiated the studies of coherent spin dynamics of rare earth ion-activated single crystals in Kazan State University in the 2000s [3].

It is well-known that the lowest states of ions with half-filled valence shells, so-called S-state ions (Fe^{3+}, Mn^{2+}, Gd^{3+}, Eu^{2+}), are characterized by certain total spin S and zero total orbital moment, so that spin-lattice and crystal-field interactions are suppressed to a certain extent [4]. Eight spin $S = 7/2$ states of trivalent gadolinium ion form the lowest spectroscopic multiplet $^8S_{7/2}$ and ideally may represent the states of three ($2^3 = 8$) qubits. Coherent manipulation of the $S = 7/2$ spin of the trivalent gadolinium ion in oxide compounds has been demonstrated previously [5, 6]. However, to the best of our knowledge, there is still no data on Rabi oscillations of Gd^{3+} incorporated into the fluorine-rich host matrix (such as $LiYF_4$), along with the demonstration of the simultaneous electron-nuclear coherence. The presence of fluorine ions in the host is both advantageous (one can utilize the ^{19}F nuclear spins as additional qubits) and disadvantageous (due to the presence of magnetic impurity, one expects the electronic coherence times to shorten significantly).

2. Results and Discussion

$LiYF_4$ crystal with rare-earth ion impurities (including neodymium and gadolinium) was grown at Kazan Federal University by the Bridgman-Stockbarger technique in argon atmosphere. Magnetic resonance measurements were done by using Bruker Elexsys E580 spectrometer operating at W band (microwave frequency $\nu = 94\,\mathrm{GHz}$) and helium flow cryostat. The electron paramagnetic resonance (EPR) spectra of Nd^{3+} ion, electron-nuclear double resonance (ENDOR) spectra of Nd^{3+} and ^{7}Li, ^{19}F nuclei have been published previously [7]. In the present article, our goal was to investigate a more promising candidate – the Gd^{3+} ion with the spin $S = 7/2$ – present as traces of uncontrolled impurity in the same crystal sample.

Firstly, we used two-pulse electron spin echo measurements (Hahn-echo sequence $\pi/2-\tau-\pi-\tau-$ echo) to detect the field-swept electron spin echo EPR spectra at low temperature, see Figure 1. There are a number of well-resolved high-intensity lines corresponding to transitions when the gadolinium spin projection M changes by one. The line positions change with temperature (which is a feature of the gadolinium ion) and agree well with the published data [8–12]. We interpret these spectra using the standard effective Hamiltonian for the ground $^{8}S_{7/2}$ multiplet of the Gd^{3+} ion occupying Y^{3+} positions with S_4 point symmetry:

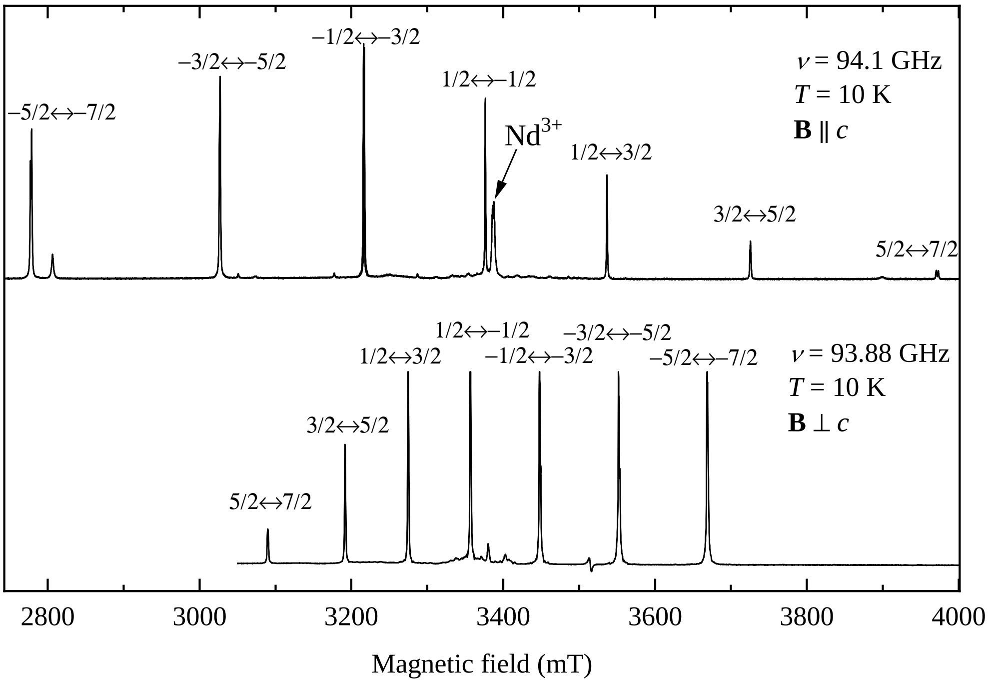

Figure 1. Field-swept electron spin echo EPR spectra of Gd^{3+} ion in $LiYF_4$ crystal at $T = 10\,\mathrm{K}$ and two directions of the magnetic field with respect to the crystal's c axis. The notation $M \leftrightarrow M'$ represents the magnetic quantum numbers of the gadolinium electronic spin involved in the particular transition. The arrow on the upper graph indicates the line belonging to Nd^{3+} ion.

$$H = \mu_{\mathrm{B}}\left(g_{\perp}B_xS_x + g_{\perp}B_yS_y + g_{\parallel}B_zS_z\right) + \frac{1}{3}b_2^0O_2^0 + \frac{1}{60}\left(b_4^0O_4^0 + b_4^4O_4^4\right) + \frac{1}{1260}\left(b_6^0O_6^0 + b_6^4O_6^4\right). \quad (1)$$

Table 1. Crystal field parameters b_p^k (GHz) and the magnetic g-factors of the Gd^{3+} ion in $LiYF_4$ crystal at 4.2 K [10].

$g_{\parallel}$	$g_{\perp}$	b_2^0	b_4^0	b_4^4	b_6^0	b_6^4
1.9900	1.9897	−2.6002	−0.0600	0.3150	0.0000	−0.0046

Due to weak mixing of the ground $^{8}S_{7/2}$ multiplet with the excited states, the Hamiltonian contains tetragonal crystal-field terms (parameterized by b_p^k parameters), in addition to the

Table 2. The EPR line positions (mT) of the Gd^{3+} ion in $LiYF_4$ crystal.

$\mathbf{B} \parallel c$		$\mathbf{B} \perp c$	
Experiment	Calculation	Experiment	Calculation
2779	2776	3090	3089
3027	3027	3192	3193
3216	3218	3275	3277
3376	3379	3356	3357
3537	3540	3448	3448
3726	3730	3552	3553
3972	3982	3669	3672

Zeeman interaction (where μ_B is Bohr magneton, $g_{\parallel}$ and $g_{\perp}$ denote magnetic g-factors for the direction of the magnetic field perpendicular and parallel to the crystal's c axis, respectively). Diagonalization of the Hamiltonian 1 was carried out using home-made software written in Matlab programming language. Our calculations with the parameters published previously [10] (see Table 1) give good agreement with the experimental EPR line positions for both field directions (Table 2). Minor discrepancy at high field and $\mathbf{B} \parallel c$ possibly originates from a small deviation of $\mathbf{B}$ direction from the c axis.

The same Hahn spin echo sequence (but where τ was varied) was used in order to obtain the spin coherence time T_2, which reached $15\,\mu$s for the low-field ($5/2 \leftrightarrow 7/2$) transition at $\mathbf{B} \perp c$ and $T = 8\,$K. The spin-lattice relaxation time measured using stimulated echo pulse sequence for the same experimental conditions equaled $T_1 = 0.4\,$ms.

Next, we measured the coherence times of the gadolinium spin in the presence of the driving microwave field (Rabi times τ_R). The sequence contained the driving pulse of variable duration t, followed by the Hahn spin echo detection sequence. The resulting spin-echo signal strength reproduced the spin projection component parallel to the field $\mathbf{B}$ at time t (spin nutations, or Rabi oscillations [13]). The nutation frequency (Rabi frequency Ω_R) corresponding to the $M \leftrightarrow M+1$ transition is proportional to the microwave field amplitude B_1:

$$\Omega_R = g\mu_B B_1 \sqrt{S\,(S+1) - M\,(M+1)}. \tag{2}$$

By controlling B_1, one can excite Rabi oscillations of various frequencies. Using different microwave field strengths, we were able to excite and detect Rabi oscillations for two Gd^{3+} transitions $-1/2 \leftrightarrow 1/2$ and $5/2 \leftrightarrow 7/2$ within the frequency range from $\Omega_R/2\pi = 0.25$ MHz to 12.8 MHz, and with τ_R reaching $4\,\mu$s. An example of the oscillations corresponding to the transition $5/2 \leftrightarrow 7/2$ is shown in Figure 2.

It is well-known that the inverse decay time τ_R^{-1} is usually linear in Ω_R, and, in the case of magnetic centers diluted in crystals, there are two main contributions to the decay: (i) spatial distribution of B_1 inside the resonator that results in dephasing of nutation signals with different Ω_R coming from different parts of the crystal sample [14]; (ii) magnetic dipole interaction between the magnetic impurity ions [15].

In the first case, the resulting decay of the oscillation amplitude is polynomial [14], while the exponential decay is a feature of (ii) [15]. In case when the impurity concentration is less than 0.1 at.%, due to intrinsic threshold in sensitivity of the detector of modern EPR spectrometers and accompanying increase in the sample size, one cannot neglect (i), but, in most cases, may

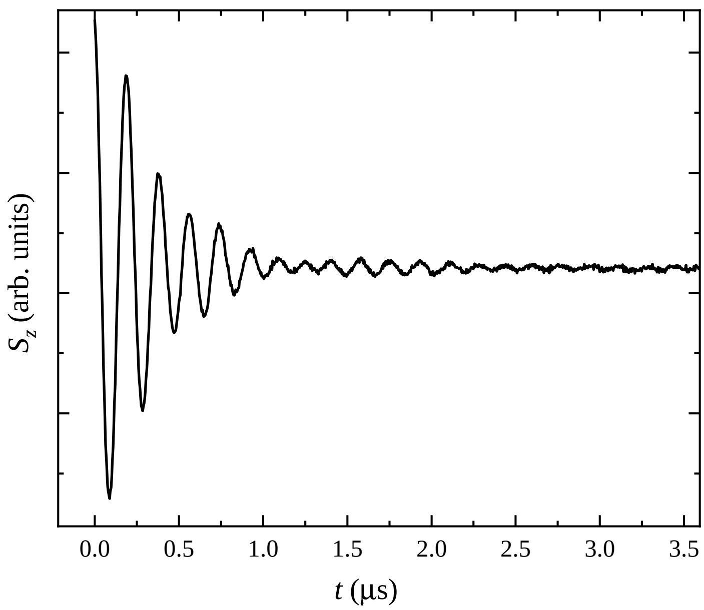

Figure 2. Rabi oscillations excited at the transition $5/2 \leftrightarrow 7/2$. $\mathbf{B} \perp c$, $T = 8\,\mathrm{K}$. Rabi frequency $\Omega_R/2\pi = 5.7\,\mathrm{MHz}$.

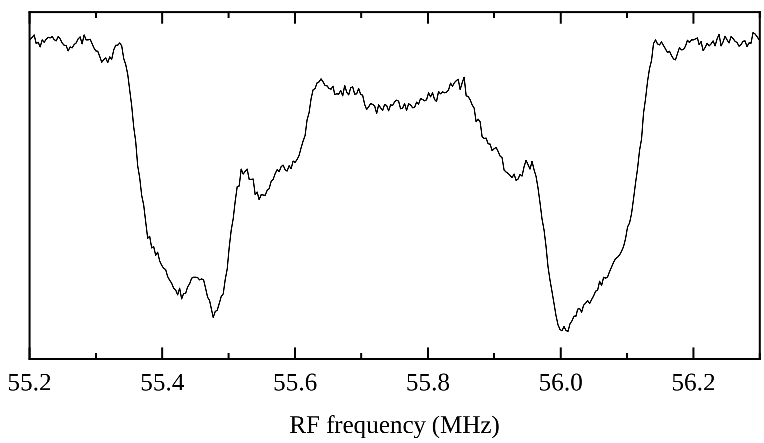

Figure 3. Mims ENDOR spectra at $-1/2 \leftrightarrow 1/2$ electronic transition in the RF frequency range corresponding to the ^{7}Li nuclear spin transition. $\mathbf{B} \parallel c$, $T = 8\,\mathrm{K}$.

neglect (ii) [16]. Our data demonstrate the polynomial decay with t which suggests that the dipolar contribution in our case was negligible.

For ENDOR experiments, we used Mims pulse sequence $\pi/2 - \tau - \pi/2 - T - \pi/2$ with an additional radiofrequency (RF) pulse π_{RF} inserted between the second and third microwave pulses. RF frequency in our setup could be swept in the range of 1–200 MHz. Magnetic field value was kept constant, corresponding to the chosen electronic transition of Gd^{3+}. Examples of the ENDOR spectra acquired for the transition $-1/2 \leftrightarrow 1/2$ are shown in Figures 3 and 4.

The observed rich structures centered at RF frequencies 55.7 and 135 MHz, respectively, correspond to ^{7}Li and ^{19}F nuclei occupying different cites in the vicinity of Gd^{3+}. The line shifts within these structures (in the range of several MHz in the case of ^{19}F) are due to the superhyperfine interaction between the electronic spin of gadolinium and nuclear spin of the ligand. The direct calculation of these shifts is complicated by the fact that there is a strong covalent contribution coming from the bonding of the rare-earth ion with the closest ligands [17].

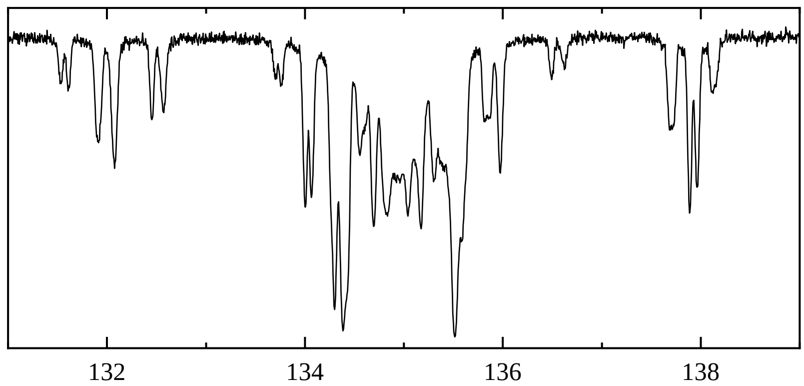

Figure 4. Mims ENDOR spectra at $-1/2 \leftrightarrow 1/2$ electronic transition in the RF frequency range corresponding to the ^{19}F nuclear spin transition. $\mathbf{B} \parallel c$, $T = 8\,$K.

3. Conclusion

This work is the first-time demonstration of the electronic and hybrid electron-nuclear spin manipulations of the $S = 7/2$ spin states of trivalent gadolinium ion diluted in $LiYF_4$ host crystal. The characteristic decay times of Rabi oscillations corresponding to the chosen $-1/2 \leftrightarrow 1/2$ and $5/2 \leftrightarrow 7/2$ transitions reach $4\,\mu$s, while the "ordinary" spin coherence time reaches $15\,\mu$s at similar experimental conditions. High-resolution pulsed Mims ENDOR spectra contain complex structures originating from the superhyperfine interactions with the nearby ^{7}Li and ^{19}F ions. The obtained results suggest a possible pulse sequence for hybrid quantum computing that would involve simultaneous selective excitation of Gd^{3+} electronic transition together with that of certain (one or more) chosen adjacent nuclear spins.

Acknowledgments

The study was funded by the subsidy allocated to Kazan Federal University for the state assignment in the sphere of scientific activities (Project No. FZSM-2024-0010).

References

1. DiVincenzo D. P., *Science* **270**, 255 (1995).

2. Bertaina S., Gambarelli S., Tkachuk A., Kurkin I. N., Malkin B., Stepanov A., Barbara B., *Nature nanotech.* **2**, 39 (2007).

3. Rakhmatullin R. M., Kurkin I. N., Mamin G. V., Orlinskii S. B., Gafurov M. R., Baibekov E. I., Malkin B. Z., Gambarelli S., Bertaina S., Barbara B., *Phys. Rev. B* **79**, 172408 (2009).

4. Abragam A., Bleaney B., *Electron paramagnetic resonance of transition ions* (OUP Oxford, 2012) 899 p.

5. Baibekov E. I., Gafurov M. R., Zverev D. G., Kurkin I. N., Rodionov A. A., Malkin B. Z., Barbara B., *Phys. Rev. B* **95**, 064427 (2017).

6. Jenkins M. D., Duan Y., Diosdado B., García-Ripoll J. J., Gaita-Ariño A., Giménez-Saiz C., Alonso P. J., Coronado E., Luis F., *Phys. Rev. B* **95**, 064423 (2017).

7. Mamin G., Murzakhanov F., Razina A., Kurkin I., Baibekov E., Orlinskii S., *IOP Conf. Series: Earth and Envir. Sci.* **282**, 012017 (2019).

8. Vaills Y., Buzare J. Y., Gesland J. Y., *Solid State Comm.* **45**, 1093 (1983).

9. Misra S. K., Kahrizi M., Mikolajczak P., Misiak L., *Phys. Rev. B* **32**, 4738 (1985).

10. Misiak L. E., Misra S. K., Mikolajczak P., *Phys. Rev. B* **38**, 8673 (1988).

11. Aminov L. K., Gafurov M. R., Korableva S. L., Kurkin I. N., Rodionov A. A., *Phys. Solid State* **59**, 564 (2017).

12. Sosin S. S., Iafarova A. F., Romanova I. V., Morozov O. A., Korableva S. L., Batulin R. G., Zhitomirsky M., Glazkov V., *JETP Lett.* **116**, 771 (2022).

13. Rabi I. I., *Phys. Rev.* **51**, 652 (1937).

14. Baibekov E., Kurkin I., Gafurov M., Endeward B., Rakhmatullin R., Mamin G., *J. Magn. Res.* **209**, 61 (2011).

15. Baibekov E. I., *JETP Lett.* **93**, 292 (2011).

16. Baibekov E. I., Gafurov M. R., Zverev D. G., Kurkin I. N., Malkin B. Z., Barbara B., *Phys. Rev. B* **90**, 174402 (2014).

17. Aminov L. K., Kurkin I. N., Malkin B. Z., *Phys. Solid State* **55**, 1343 (2013).